



ARTICLE

Solution and Analysis of the Fuzzy Volterra Integral Equations via Homotopy Analysis Method

Ali. F. Jameel^{1,*}, N. R. Anakira², A. K. Alomari³ and Noraziah H. Man¹

¹School of Quantitative Sciences, Universiti Utara Malaysia, Kedah, Sintok, 06010, Malaysia

²Department of Mathematics, Faculty of Science and Technology, Irbid National University, Irbid, 2600, Jordan

³Department of Mathematics, Faculty of Science, Yarmouk University, Irbid, 21163, Jordan

*Corresponding Author: Ali. F. Jameel. Email: alifareed@uum.edu.my

Received: 29 September 2020 Accepted: 25 February 2021

ABSTRACT

Homotopy Analysis Method (HAM) is semi-analytic method to solve the linear and nonlinear mathematical models which can be used to obtain the approximate solution. The HAM includes an auxiliary parameter, which is an efficient way to examine and analyze the accuracy of linear and nonlinear problems. The main aim of this work is to explore the approximate solutions of fuzzy Volterra integral equations (both linear and nonlinear) with a separable kernel via HAM. This method provides a reliable way to ensure the convergence of the approximation series. A new general form of HAM is presented and analyzed in the fuzzy domain. A qualitative convergence analysis based on the graphical method of a fuzzy HAM is discussed. The solutions sought by the proposed method show that the HAM is easy to implement and computationally quite attractive. Some solutions of fuzzy second kind Volterra integral equations are solved as numerical examples to show the potential of the method. The results also show that HAM provides an easy way to control and modify the convergence area in order to obtain accurate solutions.

KEYWORDS

Homotopy analysis method; convergence control parameter; fuzzy Volterra integral equations

1 Introduction

Integral equations have been used to model problems in a number of fields [1–4]. In real-world problems, inaccuracy, uncertainty and lack of information exist and are discussed both theoretically and numerically. The way to address this lack of information is to model uncertainty as fuzziness [5]. It is therefore possible to refer to fuzzy integral equations rather than to use deterministic models in the crisp domain. In order to study and solve many of the problems in applied mathematics, integral equations in fuzzy form are important, particularly for physics, for medical modelling [6]. In many applications, certain problem parameters are typically defined by a fuzzy number rather than a crisp number, and it is therefore important to establish mathematical models and numerical procedures for the proper handling of fuzzy integral equations. Numerical



approaches to fuzzy integral equations have inspired many research works in the last decade due to their use in scientific phenomena [7–11]. The existence and uniqueness of a second kind fuzzy Volterra equation solution was introduced in [12]. Among the approximate methods for fuzzy Volterra integral equations, there are the Differential Transform Method (DTM) to obtain analytical solution of linear fuzzy Volterra integral equations of second kind [13], Homotopy Perturbation Method (HPM) for solving linear and nonlinear fuzzy Volterra integral equations of second kind [14,15] and Variational Iteration Method (VIM) together with Taylor method to solve linear fuzzy Volterra integral equations of second kind [16]. The main application of fuzzy integral equations is biomathematical modelling. For example, a model based on fuzzy integral equations [16] was proposed to study the dynamics of diseases transmitted through direct contact between susceptible and infected individuals. Solving mathematical problems with approximation methods usually lead to approaches in series or polynomial functions which often have a better interpretability and this can contribute to pave the way to future processes and solutions of given problems, without the shortcoming of a suitable discretization. In the 90s, Liao introduced a new approximation approach called homotopy analysis method [17]. The approximate solution is obtained as an infinite series function that has been shown to converge to the exact solution in many mathematical problems involving engineering applications [18–22]. The homotopy, a fundamental concept in topology, is a landmark of the approximation methods, since it provides more flexibility in handling the equations and their solution [23]. The validity of HAM depends on homotopy topology, regardless of the physical parameters. It is worth recalling that the Adomian Decomposition Method (ADM) and the VIM are non-perturbation techniques, which do not depend on a series of physical parameters, but such non-perturbation techniques in some cases do not guarantee the convergence of the solution series [24]. The HAM also allows to select the proper base function without any constraint to approximate the solution of some nonlinear problems [25].

The difference between HAM and other approximation methods is the auxiliary convergence control parameter, denoted by h , that can optimize and rate the convergence of the method per order of solution [26]. In HAM the selections of proper initial approximation, operator and auxiliary function with the optimal value of h allows to solve the deformation equations and develop a solution series [20].

To control the error of HAM solution, there is a convergence-control parameter, whose value, if properly selected, can lead to an accurate convergent series or faster convergence [27]. Van Gorder et al. [28] discussed the application of HAM for nonlinear ordinary differential equation and the effectiveness of a suitable choice of initial approximation, auxiliary linear operator, auxiliary function and convergence control parameter. There are several methods to obtain the best value of the convergence-control parameter such as control of residual errors, minimization of error functional and optimal selection of the homotopy of auxiliary function which were introduced and suggested for the approximate solution of semi-linear elliptic equation in [29]. Moreover, an algorithm was proposed in [30] to optimize the solution of singular and integral equation of first kind via HAM by computing the optimal auxiliary control parameter value.

HAM has been used to solve several types of problems in crisp and fuzzy domains, e.g., fluid flow and heat transfer problems [31], fractional differential equations involving biological models [32], system of nonlinear ordinary differential equations describing HIV infection models [33], Abel's integral equations of the first kind [34], fuzzy boundary value problem [35] and fuzzy delay differential equation [36].

The present work deals with the approximate solution of fuzzy Volterra integral equations of second kind, since to the best knowledge of the authors no study has been carried out by formulating the general concept of HAM from the crisp domain to the fuzzy domain for solving such class problems.

The paper is structured as follows. The Volterra integral equations of the second kind with the defuzzification details are recalled in the next section. A new description of the fuzzy HAM general formula is presented in Section 3, where a convergence analysis is also outlined. In Section 4, some test problems are considered and the numerical results discussed. Finally, there is a short conclusion that includes a summary of this work. Note that some of the basic fuzzy definitions, remarks and concepts not described in this paper are well-known. Notions of fuzzy level sets, fuzzy numbers and their operations, fuzzy functions, fuzzy Zadeh extension theory and integral of fuzzy functions can be easily retrieved from the literature, e.g., [9,37–41].

2 Fuzzy Volterra Integral Equation

The general fuzzy version of the standard second kind Volterra integral equation [9] is defined below:

$$\tilde{x}(t) = \tilde{f}(t) + \tilde{\lambda} \int_a^t \tilde{k}(t, s, \tilde{x}(s)) ds, \tag{1}$$

where $\tilde{\lambda}$ is a positive fuzzy parameter, \tilde{k} is an arbitrary function called the kernel of the integral Eq. (1) defined over square $G: [a, b] \times [a, b]$, $\tilde{k} = 0$, $a \leq s, t \leq b$, $s > t$ and $\tilde{f}(t)$ is a given fuzzy function of $t \in [a, b]$ with $\tilde{x}(s)$ is the unknown fuzzy function to be determined.

Eq. (1) follows the properties of the standard second kind Volterra integral equation in crisp domain by means of defuzzification according to [9]. Hence, Eq. (1) with the fuzzy parametric forms are given as follows:

$$\tilde{x}(t; r) = \tilde{f}(t; r) + \tilde{\lambda}(r) \int_a^t \tilde{k}(t, s, \tilde{x}(s; r); r) ds, \tag{2}$$

where

$$\begin{cases} \tilde{x}(t) = \tilde{x}(t; r) = [\underline{x}(t; r), \overline{x}(t; r)], \\ \tilde{f}(t) = \tilde{f}(t; r) = [\underline{f}(t; r), \overline{f}(t; r)], \\ \tilde{\lambda} = \tilde{\lambda}(r) = [\underline{\lambda}(r), \overline{\lambda}(r)], \\ \tilde{k}(t, s, \tilde{x}(s)) = \tilde{k}(t, s, \tilde{x}(s); r) = [\underline{k}(t, s, \underline{x}(s; r); r), \overline{k}(t, s, \overline{x}(s; r); r)], \\ \tilde{x}(s) = \tilde{x}(s; r) = [\underline{x}(s; r), \overline{x}(s; r)]. \end{cases} \tag{3}$$

with $0 \leq r \leq 1$. By using Eq. (3), the solution of Eq. (1) can be obtained by solving the following two integral equations:

$$\begin{cases} \underline{x}(t; r) = \underline{f}(t; r) + \underline{\lambda}(r) \int_a^x \underline{k}(t, s, \underline{x}(s; r); r) ds \\ \overline{x}(t; r) = \overline{f}(t; r) + \overline{\lambda}(r) \int_a^x \overline{k}(t, s, \overline{x}(s; r); r) ds \end{cases} \tag{4}$$

The sufficient conditions for the existence of a unique solution to Eq. (2) are given and proved in [11].

3 General Fuzzy HAM

The crisp form of HAM was introduced in [42]. To describe the dynamic of the HAM under homotopy theory in the fuzzy domain, we start off with:

$$\mathcal{N}[\tilde{x}(t; r)] = 0, \quad (5)$$

where \mathcal{N} is a nonlinear operator, t is an independent variable and, $\tilde{x}(t; r)$ is an unknown fuzzy function. According to [14], the zero-order fuzzy deformation HO for all $r \in [0, 1]$:

$$HO(t; p; r) = (1 - p)L[\tilde{\theta}(t; p; r) - \tilde{x}_0(t; r)] - p\tilde{h}(r)H(t)\mathcal{N}[\tilde{\theta}(t; p; r)], \quad (6)$$

where $p \in [0, 1]$ is an embedding parameter, $\tilde{h}(r) \neq 0$ is a convergence-control parameters per each r level sets. Function $H(t) \neq 0$ is an auxiliary function, L is an auxiliary linear operator, $\tilde{x}_0(t; r)$ is the fuzzy initial guess of $\tilde{x}(t; r)$ and $\tilde{\theta}(t; p; r)$ is the auxiliary function that should satisfy the initial conditions. It should be noted that the $\tilde{h}(r)$ and $H(t)$ are necessary to the HAM series solution rate of the convergence [17]. The parameter p changes from 0 to 1 to generate series solution such that when $p = 0$, one has

$$HO(t; 0; r) = L[\tilde{\theta}(t; 0; r) - \tilde{x}_0(t; r)] = 0, \quad (7)$$

while if $p = 1$, one gets

$$HO(t; 1; r) = p\tilde{h}(r)H(t)\mathcal{N}[\tilde{\theta}(t; 1; r)] = 0. \quad (8)$$

Thus, by imposing

$$HO(t; p; r) = 0, \quad (9)$$

It is

$$(1 - p)L[\tilde{\theta}(t; p; r) - \tilde{x}_0(t; r)] = p\tilde{h}(r)H(t)\mathcal{N}[\tilde{\theta}(t; p; r)]. \quad (10)$$

From [13], if $p = 0$ and $p = 1$, the homotopy equations becomes

$$\begin{cases} \tilde{\theta}(t; 0; r) = \tilde{x}_0(t; r), \\ \tilde{\theta}(t; 1; r) = \tilde{x}(t; r). \end{cases}, \quad (11)$$

As p changes from 0 to 1, the fuzzy solution $\tilde{\theta}(t; p; r)$ varies from the initial guess $\tilde{x}_0(t; r)$ to the HAM solution $\tilde{x}(t; r)$. By expanding $\tilde{\theta}(t; 0; r)$ as a Taylor series in terms of p , we can yield the series solution in the following form:

$$\tilde{\theta}(t; p; r) = \tilde{x}_0(t; r) + \sum_{m=1}^{\infty} \tilde{x}_m(t; r)p^m, \quad (12)$$

where

$$\tilde{x}_m(t; r) = \frac{1}{m!} \frac{\partial^m \tilde{\theta}(t; p; r)}{\partial p^m} \Big|_{p=0}. \tag{13}$$

The auxiliary linear operator L , the initial guess $\tilde{x}_0(t; r)$, the convergence control $\tilde{h}(r)$ and the auxiliary function $H(t)$ are very important for the best homotopy series solution. Note that if $p = 1$ then we have

$$\tilde{\theta}(t; 1; r) = \tilde{x}_0(t; r) + \sum_{m=1}^{\infty} \tilde{x}_m(t; r) p^m, \tag{14}$$

which is one of the solutions of the given equation to be solved by HAM. Notice that if all the values of $\tilde{h}(r) = -1$ and $H(t) = 1$ then Eq. (10) takes the form:

$$(1-p)L[\tilde{\theta}(t; 1; r) - \tilde{x}_0(t; r)] + p\mathcal{N}[\tilde{\theta}(t; 1; r)] = 0, \tag{15}$$

which represents the homotopy perturbation method (HPM), implying that HPM is a special case of HAM [43]. From Eq. (10) the governing equations can be deduced from the zero-order deformation Eq. (12) by defining the vectors:

$$\vec{\tilde{x}}_i(t; r) = \{\tilde{x}_0(t; r), \tilde{x}_1(t; r), \dots, \tilde{x}_m(t; r)\}. \tag{16}$$

By deriving with respect to p both sides of Eq. (10) m times, at $p = 0$, and after that dividing them by $m!$, we obtain the m th-order deformation equation

$$L[\vec{\tilde{x}}_m(t; r) - \chi_m \vec{\tilde{x}}_{m-1}(t; r)] = \tilde{h}(r) \mathcal{R}_m(\vec{\tilde{x}}_{m-1}(t; r)), \tag{17}$$

where

$$\mathcal{R}_m(\vec{\tilde{x}}_{m-1}(t; r)) = \frac{1}{(m-1)!} \frac{\partial^{m-1} N[\tilde{\theta}(t; p; r)]}{\partial p^{m-1}} \Big|_{p=0}, \quad \chi_m = \begin{cases} 0, & m \leq 1 \\ 1, & m > 0 \end{cases}. \tag{18}$$

4 Fuzzy HAM for Fuzzy Volterra Integral Equations

In this section, the HAM solution of fuzzy Volterra integral equations is described in some steps.

Construct the zeroth-order deformation for Eq. (1) for all $r \in [0, 1]$ as:

$$(1-p)L[\tilde{x}(t; p; r) - \tilde{f}(t; r)] = p\tilde{h}(r) \left[\tilde{x}(t; p; r) - \tilde{f}(t; r) - \tilde{\lambda}(r) \int_a^t \tilde{k}(t, s, \tilde{x}(s; p; r); r) ds \right]. \tag{19}$$

Set the values of $p = 0$ and $p = 1$, implying

$$\begin{cases} \tilde{x}(t; 0; r) = \tilde{f}(t; r), \\ \tilde{x}(t; 1; r) = \tilde{x}(t; r). \end{cases} \tag{20}$$

From Eq. (20), it follows that the fuzzy initial guess $\tilde{x}_0(t; r)$ can be selected from $\tilde{f}(t; r)$ as there are no restrictions to select the proper HAM initial guess to obtain the suitable solution of any given equation [17]. According to Section 3, the Taylor series in terms of p for $\tilde{x}(t; p; r)$ is:

$$\tilde{X}(t; p; r) = \tilde{x}(t; 0; r) + \sum_{m=1}^{\infty} \frac{\tilde{x}_m(t; r; \tilde{h}(r))}{m!} p^m, \quad (21)$$

where $\tilde{x}_m(t; r; \tilde{h}(r)) = \left. \frac{1}{m!} \frac{\partial^m \tilde{x}_m(t; r; p; \tilde{h}(r))}{\partial p^m} \right|_{p=0}$. Now for $p = 1$ in Eq. (21) the m th-order deformation equation is obtained:

$$\tilde{X}(t; r) = \tilde{f}(t; r) + \sum_{m=1}^{\infty} \frac{\tilde{x}_m(t; r; \tilde{h}(r))}{m!}. \quad (22)$$

From the m th-order deformation equation

$$\begin{aligned} \tilde{x}_m(t; r) = \chi_{m-1} \tilde{x}_{m-1}(t; r) + \tilde{h}(r) & \left[\tilde{x}_{m-1}(t; r) - \int_0^t (\tilde{\lambda}(r) \tilde{k}(t, s, \tilde{x}_{m-1}(s; r); r)) ds \right. \\ & \left. - (1 - \chi_{m-1}) \tilde{f}(t; r) \right], \end{aligned} \quad (23)$$

$$\chi_m = \begin{cases} 0, & m \leq 1 \\ 1, & m > 0 \end{cases},$$

one obtains

$$\tilde{x}_1(t; r; \tilde{h}(r)) = \tilde{h}(r) \tilde{x}_0(t; r) - \tilde{h}(r) \tilde{f}(t; r) - \left[\tilde{h}(r) \int_0^t (\tilde{\lambda}(r) \tilde{k}(t, s; \tilde{x}_0(s; r); r)) ds \right], \quad (24)$$

where $\tilde{x}_0(t; r)$ is the initial guess obtained from $\tilde{f}(t; r)$ and for $m \geq 2$, we have:

$$\tilde{x}_m(t; r; \tilde{h}(r)) = (1 + \tilde{h}(r)) \tilde{x}_{m-1}(t; r; \tilde{h}(r)) - \left[\tilde{h}(r) \int_0^t (\tilde{\lambda}(r) \tilde{k}(t, s, \tilde{x}_{m-1}(t; r; \tilde{h}(r)); r)) ds \right]. \quad (25)$$

Then the fuzzy HAM series solution can be written in the following form:

$$\tilde{X}(t; r; \tilde{h}(r)) = \tilde{x}_0(t; r) + \sum_{m=1}^{\infty} \tilde{x}_m(t; r; \tilde{h}(r)) = \begin{cases} \underline{x}_0(t; r) + \sum_{m=1}^{\infty} \underline{x}_m(t; r; \underline{h}(r)), \\ \bar{x}_0(t; r) + \sum_{m=1}^{\infty} \bar{x}_m(t; r; \bar{h}(r)). \end{cases} \quad (26)$$

The convergence of Eq. (26) depends on selecting a suitable value of $\tilde{h}(r)$. The solution is therefore obtained in series form (homotopy solution series):

$$\tilde{X}(t; r) = \lim_{m \rightarrow \infty} \sum_{m=0}^{\infty} \tilde{x}_m(t; r). \tag{27}$$

It is worth noticing that since the defuzzification leads to a system of crisp equations, the theoretical achievements on the convergence in [30] can be adapted.

5 Dynamics of Fuzzy HAM Convergence

As mentioned before, the convergence of the approximate solution of Eq. (1) relies on the value of the parameter $\tilde{h}(r)$. Therefore, the value of $\tilde{h}(r)$ should be sought to provide sufficient accuracy for a certain order of the HAM series solution. The procedure is to define first Eq. (26) in residual form:

$$\tilde{R}(t; r; \tilde{h}(r)) = \tilde{X}(t; r; \tilde{h}(r)) - \tilde{f}(t) - \tilde{\lambda} \int_a^t \tilde{k}(t, s, \tilde{X}(t; r; \tilde{h}(r))) ds. \tag{28}$$

then to use the least square method to optimize the values of $\tilde{h}(r)$ such that:

$$\tilde{S}(t; r; \tilde{h}(r)) = \int_a^t (\tilde{R}(t; r; \tilde{h}(r)))^2 dt. \tag{29}$$

After that, the nonlinear equation coming from Eq. (29) in terms of $\tilde{h}(r)$ for any $r \in [0, 1]$ is deduced such that:

$$\frac{\partial \tilde{S}(t; r; \tilde{h}(r))}{\partial \tilde{h}(r)} = 0 \rightarrow \begin{cases} \frac{\partial \underline{\tilde{S}}(t; r; \underline{\tilde{h}}(r))}{\partial \underline{\tilde{h}}(r)} = 0 \\ \frac{\partial \overline{\tilde{S}}(t; r; \overline{\tilde{h}}(r))}{\partial \overline{\tilde{h}}(r)} = 0 \end{cases}. \tag{30}$$

Finally, the equation is solved for $\tilde{h}(r)$ in each fuzzy level set to obtain the best value of \tilde{h} to be replaced in Eq. (26), in order to rate the convergence of the HAM solution. Hence, one needs to estimate the best value of $\tilde{h}(r)$ to get the best approximate solution $\tilde{X}(t; r; \tilde{h}(r))$. This can be done by plotting the h -curves for all $r \in [0, 1]$. These curves can help to find the region \mathbb{C} which contains the best values of $\tilde{h}(r) \in \mathbb{C}$. If there exist $c_0 \in [0, T]$, by plotting the quantities $\tilde{R}(t; r; \tilde{h}(r))$, $\tilde{X}_m(x, \tilde{h}(r); r)$, $\tilde{X}'_m(c_0; r; \tilde{h}(r))$, $\tilde{X}''_m(c_0; r; \tilde{h}(r))$ and so on for $-2 < \tilde{h}(r) < 0$, it is possible to find the valid region \mathbb{C} . The latter is known to be delimited by the line nearly parallel to the horizontal axis [17]. According to [35,36] the best value of \tilde{h} can be selected from the fuzzy level set $r = r_0$ with highest accuracy and then replaced in the remainder for the optimal upper and lower bound solutions of Eq. (1).

The HAM for seeking the approximate solution of Eq. (1) can be summarized in the following algorithm.

Step 1: Set the initial guess $\tilde{x}_0(t; r) = \tilde{x}_0$ ($\tilde{x}_0 = [\underline{x}_0, \bar{x}_0]$).

Step 2: Set the value of $\tilde{\lambda}(r) = [\underline{\lambda}(r), \bar{\lambda}(r)]$.

Step 3: Set number of terms, s.t. $i = 1, 2, \dots, j$.

Step 4: Set $i = i + 1$ and for $i = 1$ to $i \leq j$ evaluate

$$\tilde{x}_i(t; r) = \chi_{i-1} \tilde{x}_{i-1}(t; r) + \tilde{h}(r) \left[\tilde{x}_{i-1}(t; r) - \int_0^t (\tilde{\lambda}(r) \tilde{k}(t, s, \tilde{x}_{i-1}(s; r); r)) ds - (1 - \chi_{i-1}) \tilde{f}(t; r) \right].$$

Step 5: Compute

$$\tilde{X}(t; r; \tilde{h}(r)) = \sum_{k=0}^j \tilde{x}_{i-1}(t; r). \quad (*)$$

Step 6: Set the fixed value of $r_0 \in [0, 1]$ and $t \in [a, b]$; evaluate

$$\tilde{h}(r_0) = \frac{\partial \tilde{X}(t; r_0; \tilde{h}(r_0))}{\partial \tilde{h}(r_0)},$$

then plot the h -curve ($-2 \leq h \leq 0$).

Step 7: Define the residual form in Eq. (28) and use Eqs. (29)–(30) to find the best value of $\tilde{h}(r_0)$; then substitute the values of $\tilde{h}(r_0)$ in Eq. (*) to detect the optimal value of $\tilde{h}(r_0)$.

Step 8: Replace again the optimal value of $\tilde{h}(r)$ for the lower and upper level in Eq. (*).

6 Application Examples

In this section application examples are presented. For the remainder of this work, \tilde{Er} and \widetilde{MEr} will denoted the absolute error and the mean error respectively, defined as follows:

$$\tilde{Er}(t, r; \tilde{h}) = \left| \widetilde{XX}(t; r) - \tilde{X}(t; r; \tilde{h}) \right| = \begin{cases} \left| \underline{XX}(t; r) - \underline{X}(t; r; \tilde{h}) \right| \\ \left| \overline{XX}(t; r) - \overline{X}(t; r; \tilde{h}) \right| \end{cases} \quad (31)$$

$$\widetilde{MEr}(t, r; \tilde{h}) = \frac{\underline{Er}(t, r; \tilde{h}) + \overline{Er}(t, r; \tilde{h})}{2} \quad (32)$$

Example 6.1: Consider the following linear fuzzy Volterra integral equation [13]:

$$\tilde{x}(t) = \tilde{f}(t) + \int_0^x (t-s) \tilde{x}(s) ds, \quad (33)$$

where $\tilde{f}(t; r) = \left(1 - t - \frac{t^2}{2}\right) [r, 2 - r]$ and its exact solution

$$\widetilde{XX}(t; r) = [r, 2 - r] (1 - \sinh(t)). \quad (34)$$

The HAM formulation (see Section 5) for Eq. (33) is:

$$\begin{aligned} \tilde{x}_m(t; r) = & \chi_{m-1} \tilde{x}_{m-1}(t; r) + \tilde{h}(r) \left[\tilde{x}_{m-1}(t; r) - \int_0^t (t-s) \tilde{x}_{m-1}(s; r) ds \right. \\ & \left. - (1 - \chi_{m-1}) \left(1 - t - \frac{t^2}{2} \right) [r, 2-r] \right], \end{aligned} \tag{35}$$

where the initial guess $\tilde{x}_0(t; r) = \tilde{f}(t; r)$. By following the analysis in Section 4 and according to [36], for fixed values of the r -level set, namely $r = 0.6$, the $\tilde{h}(r)$ -curves of fifth-order fuzzy HAM upper and lower bound solutions $\tilde{X}(t, \tilde{h}(r); r)$ for Eq. (33) are shown in the following figures.

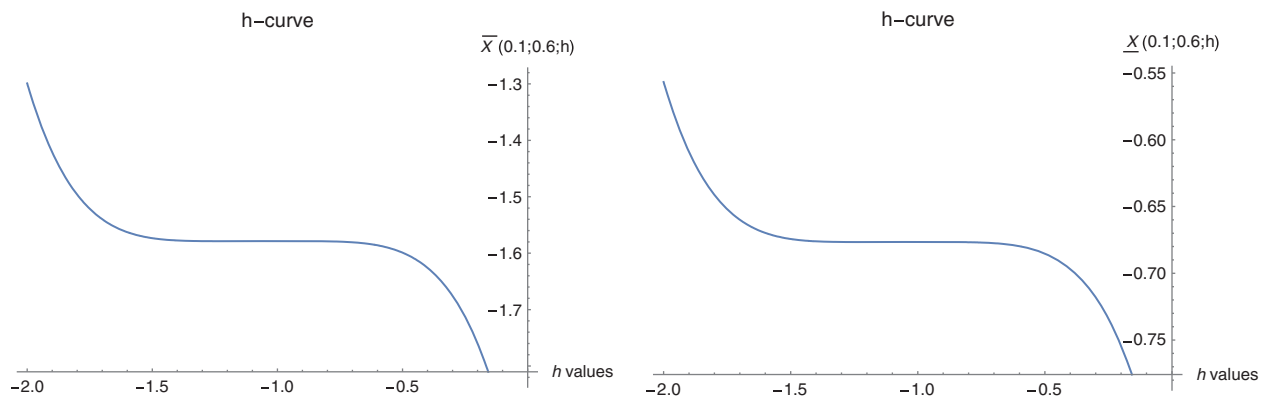


Figure 1: Fifth-order fuzzy HAM solution $\tilde{h}(r)$ -curves of Eq. (33) at $r = 0.6$

From Fig. 2, the range of the valid values of \tilde{h} (graph line almost parallel to the horizontal axis) for the fifth-order fuzzy HAM solution is $-1.5 \leq \tilde{h}(0.6) \leq -0.6$. From Eq. (30) the best valid values of \tilde{h} are listed in Tab. 1.

Fig. 3 shows the absolute errors defined in Eq. (31) of the fifth-order fuzzy HAM solution for the values $\tilde{h}(r)$ in Tab. 1.

To be more precise regarding the convergence of HAM, if the values of $\tilde{h}(0.6)$ are selected such that $\tilde{h}(0.6) \notin [-1, 5, -0.6]$, e.g., $\tilde{h}(0.6) = 1$ or $\tilde{h}(0.6) = -3$, the plots in Fig. 3 are obtained.

From Fig. 3, one can easily deduce that for values of $\tilde{h}(r)$ not in the convergence region, one obtains a divergent HAM solution. From Fig. 2, one can notice that $\tilde{h}_2 = -1.0039263129319256$ is the optimal value of the convergence control parameters among those in Tab. 1. Therefore, Tabs. 2–5 will display the solutions and accuracy of Eq. (33) via fifth-order HAM as follows.

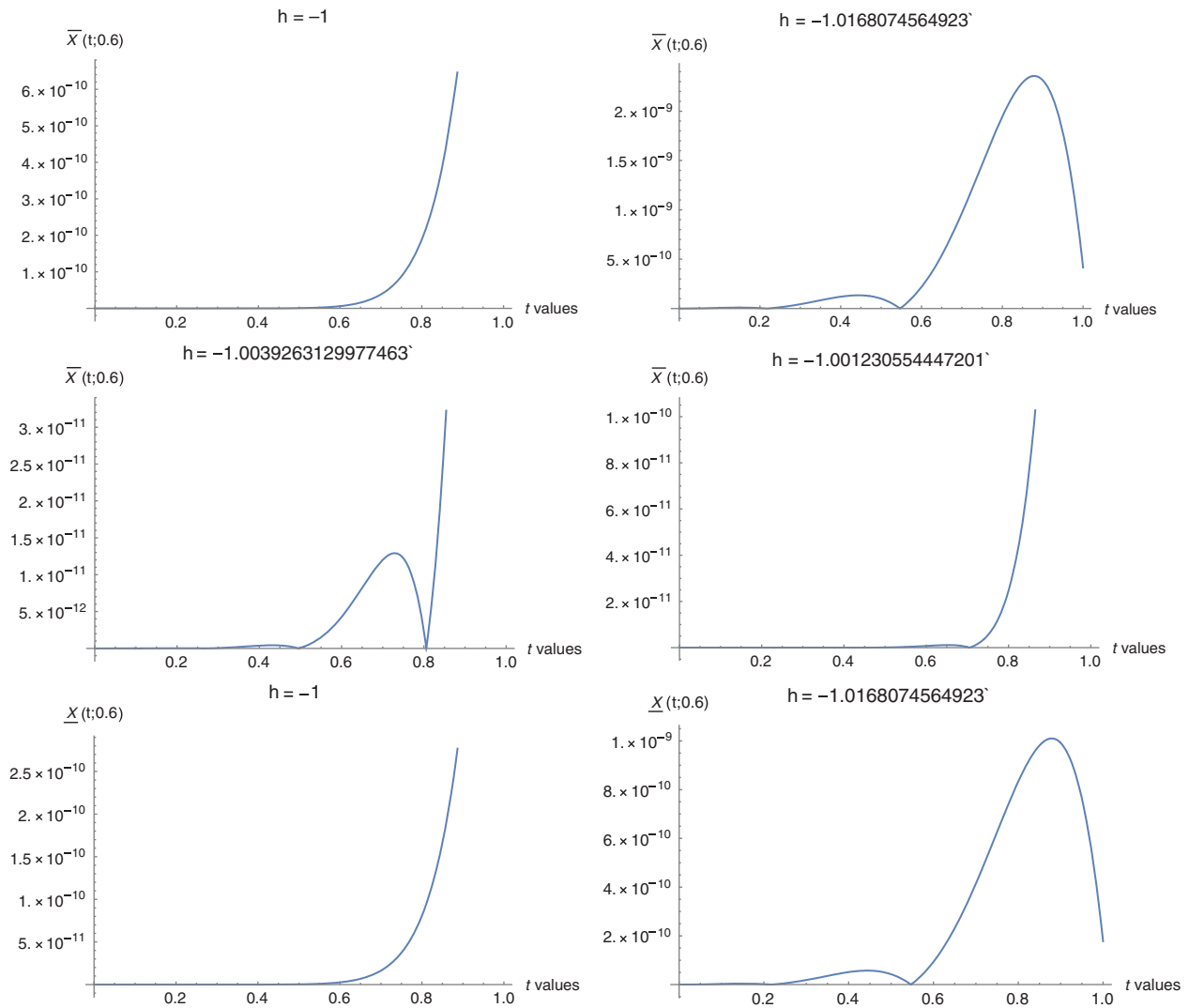


Figure 2: Fifth-order fuzzy HAM solutions accuracy for different values of $\tilde{h}(0.6)$

Table 1: Best values of the convergence control parameter of fifth-order fuzzy HAM solution of Eq. (33) at $r = 0.6$

$\underline{X}(t, \underline{h}(0.6); 0.6)$	$\underline{h}_1 \rightarrow -1.0168074564923$	$\underline{h}_2 \rightarrow -1.0039263129319256$	$\underline{h}_3 \rightarrow -1.0012305544466953$
$\overline{X}(t, \overline{h}(0.6); 0.6)$	$\overline{h}_1 \rightarrow -1.0168074564923$	$\overline{h}_2 \rightarrow -1.0039263129977463$	$\overline{h}_3 \rightarrow -1.001230554447201$

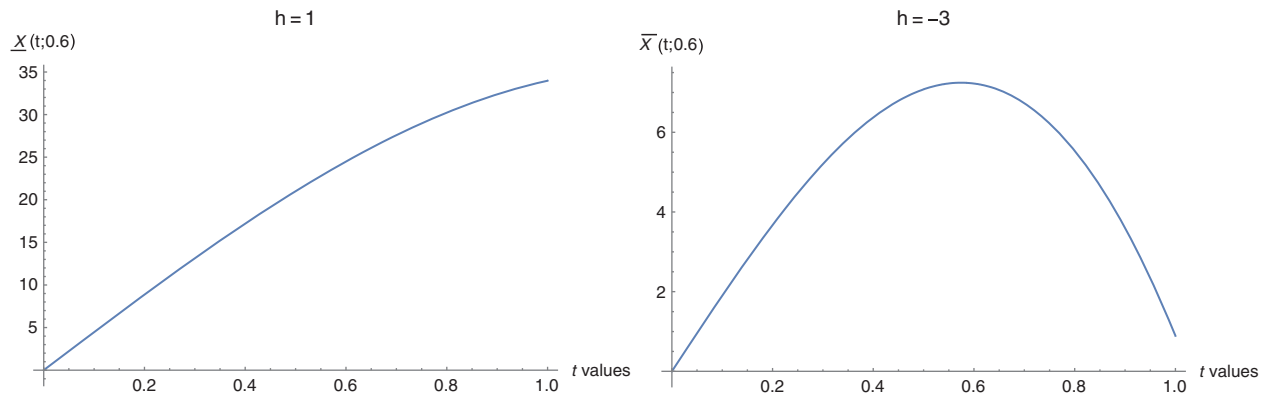


Figure 3: Fifth-order fuzzy HAM solutions for two different values of $\tilde{h}(0.6)$

Table 2: Fifth-order HAM lower solution and accuracy of Eq. (33) at $t = 1$ and $\tilde{h} = \underline{h}_2$ for all $r \in [0, 1]$

r	$\underline{X}(t; r; -1)$	$\underline{XX}(t; r)$	$\underline{Er}(t, r; -1)$
0	0	0	0
0.2	-0.03504023911402382	-0.03504023872876027	$1.155790504969722 \times 10^{-9}$
0.4	-0.07008047822804765	-0.07008047745752055	$1.155790504969722 \times 10^{-9}$
0.6	-0.10512071734207154	-0.10512071618628084	$1.155790504969722 \times 10^{-9}$
0.8	-0.14016095645609530	-0.14016095491504110	$1.155790504969722 \times 10^{-9}$
1	-0.17520119557011918	-0.17520119364380138	$1.155790504969722 \times 10^{-9}$

Table 3: Fifth-order HAM lower solution and accuracy for Eq. (33) at $t = 1$ and $\tilde{h} = \underline{h}_2$ for all $r \in [0, 1]$

r	$\underline{X}(t; r; \underline{h}_2)$	$\underline{XX}(t; r)$	$\underline{Er}(t, r; \underline{h}_2)$
0	0	0	$1.671944666048475 \times 10^{-10}$
0.2	-0.03504023867302880	-0.035040238728760276	$1.671944666048475 \times 10^{-10}$
0.4	-0.07008047734605760	-0.070080477457520550	$1.671944666048475 \times 10^{-10}$
0.6	-0.10512071601908646	-0.105120716186280840	$1.671944666048475 \times 10^{-10}$
0.8	-0.14016095469211520	-0.140160954915041100	$1.671944666048475 \times 10^{-10}$
1	-0.17520119336514406	-0.175201193643801380	$1.671944666048475 \times 10^{-10}$

Table 4: Fifth-order HAM upper solution and accuracy for Eq. (33) at $t = 1$ and $h = 1$ for all $r \in [0, 1]$

r	$\overline{X}(t; r; -1)$	$\overline{XX}(t; r)$	$\overline{Er}(t, r; -1)$
0	-0.35040239114023775	-0.35040238728760276	$2.696844247918051 \times 10^{-9}$
0.2	-0.31536215202621450	-0.31536214855884250	$2.696844247918051 \times 10^{-9}$
0.4	-0.28032191291219066	-0.28032190983008220	$2.696844247918051 \times 10^{-9}$
0.6	-0.24528167379816626	-0.24528167110132190	$2.696844247918051 \times 10^{-9}$
0.8	-0.21024143468414302	-0.21024143237256165	$2.696844247918051 \times 10^{-9}$
1	-0.17520119557011887	-0.17520119364380138	$2.696844247918051 \times 10^{-9}$

Table 5: Fifth-order HAM upper solution and accuracy for Eq. (33) at $t = 1$ and $h = \bar{h}_2$ for all $r \in [0, 1]$

r	$\bar{X}(t; r; \bar{h}_2)$	$\bar{XX}(t; r)$	$\bar{Er}(t; r; \bar{h}_2)$
0	-0.35040238673028773	-0.35040238728760276	$3.901206302447946 \times 10^{-10}$
0.2	-0.31536214805725904	-0.31536214855884250	$3.901206302447946 \times 10^{-10}$
0.4	-0.28032190938423040	-0.28032190983008220	$3.901206302447946 \times 10^{-10}$
0.6	-0.24528167071120120	-0.24528167110132190	$3.901206302447946 \times 10^{-10}$
0.8	-0.21024143203817297	-0.21024143237256165	$3.901206302447946 \times 10^{-10}$
1	-0.17520119336514386	-0.17520119364380138	$3.901206302447946 \times 10^{-10}$

From Figs. 4, 5 one can notice that the fifth-order fuzzy HAM solutions of Eq. (31) are in the form of fuzzy numbers for any $r \in [0, 1]$ and any $t \in [0, 1]$.

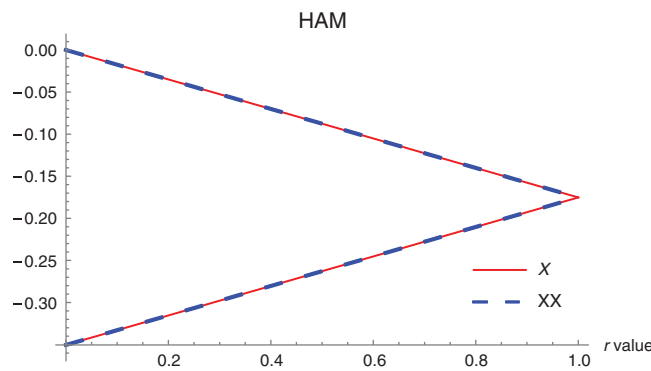


Figure 4: Fifth-order fuzzy HAM solution for $h = \tilde{h}_2$ and exact solution of Eq. (33) at $t = 1$, $r \in [0, 1]$

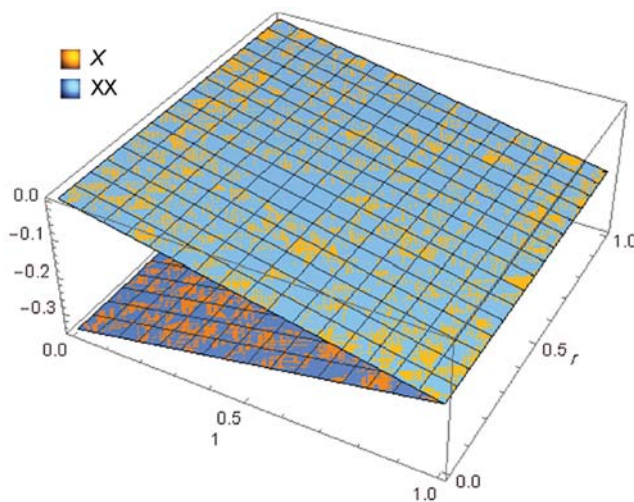


Figure 5: Fifth-order HAM solution for $h = \tilde{h}_2$ and the exact solution of Eq. (33) for $t \in [0, 1]$ and $r \in [0, 1]$

Example 6.2: Consider the following linear fuzzy Volterra integral equation [16]:

$$\tilde{x}(t) = [r, 2 - r] \cos(t) + \int_a^x e^{t-s} \tilde{x}(s) ds, \tag{36}$$

The exact solution of Eq. (36) is given by

$$\tilde{X}(t; r) = [r, 2 - r] \left(\frac{3}{5} \cos(t) + \frac{1}{5} \sin(t) + \frac{2}{5} e^{2t} \right). \tag{37}$$

The HAM formulation of Eq. (36) is:

$$\tilde{x}_m(t; r) = \chi_{m-1} \tilde{x}_{m-1}(t; r) + \tilde{h}(r) \left[\tilde{x}_{m-1}(t; r) - \int_0^t (e^{t-s} \tilde{x}_{m-1}(s; r)) ds - (1 - \chi_{m-1}) \cos(t) [r, 2 - r] \right], \tag{38}$$

where the initial guess is assumed to be $\tilde{x}_0(t; r) = [r, 2 - r]$. The $\tilde{h}(r)$ -curves of sixth-order fuzzy HAM upper and lower bound solutions at $r = 0.8$ for Eq. (36) are shown in Fig. 6.

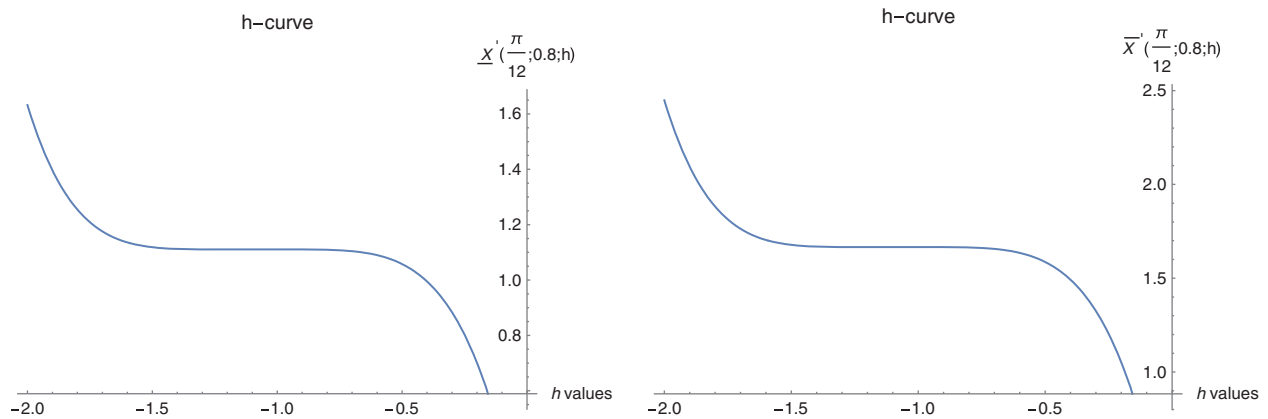


Figure 6: $\tilde{h}(r)$ -curves of the sixth-order fuzzy HAM solution of Eq. (36) at $r = 0.8$

The valid values of \tilde{h} from Fig. 6 are clearly in the range $-1.5 \leq \tilde{h}(0.8) \leq -0.6$. From Eq. (30) the best valid values of \tilde{h} are listed in Tab. 6.

Table 6: Best values of the convergence control parameter of sixth-order fuzzy HAM solution of Eq. (36) at $r = 0.8$

$\underline{X}(t, \underline{h}(0.8); 0.8)$	$\underline{h}_1 \rightarrow -1.0794786559433383$	$\underline{h}_2 \rightarrow -1.038596279179304$	$\underline{h}_3 \rightarrow -1.0212191766736773$
$\overline{X}(t, \overline{h}(0.8); 0.8)$	$\overline{h}_1 \rightarrow -1.0794786558283624$	$\overline{h}_2 \rightarrow -1.0385962794446666$	$\overline{h}_3 \rightarrow -1.0212191765124560$

From Fig. 7, one can see that the optimal value of the convergence control parameters in Tab. 6 is \tilde{h}_2 . Tab. 7 and 8 show the sixth-order HAM approximate solution of Eq. (36) for $t = [0, \frac{\pi}{8}]$ and $r \in [0, 1]$.

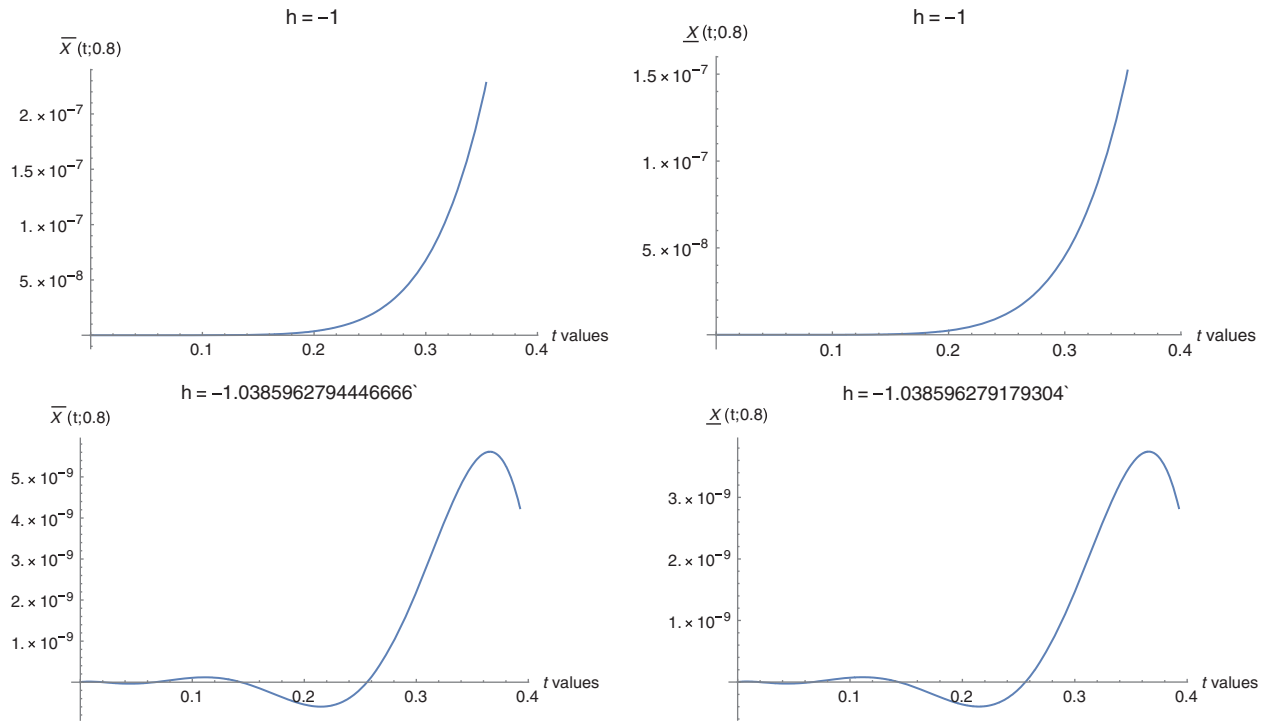


Figure 7: Sixth-order fuzzy HAM solution accuracy for some values of \tilde{h} (0.8), $t \in [0, \frac{\pi}{8}]$

Table 7: Sixth-order HAM solution of Eq. (36) at $t = \frac{\pi}{8}$ and $h = -1$ for $r \in [0, 1]$

r	$\overline{XX}(t; r)$	$\overline{X}(t; r; -1)$	$\underline{X}(t; r; -1)$	$\underline{XX}(t; r)$
0.	3.0163528525499923	3.0163520424834314	0.	0.
0.1	2.8655352099224927	2.8655344403592595	0.15081760212417156	0.15081764262749964
0.2	2.7147175672949930	2.7147168382350886	0.30163520424834310	0.3016352852549993
0.34	2.5638999246674934	2.5638992361109163	0.45245280637251467	0.4524529278824989
0.4	2.4130822820399940	2.4130816339867460	0.6032704084966862	0.6032705705099985
0.5	2.2622646394124940	2.2622640318625730	0.7540880106208577	0.7540882131374981
0.6	2.1114469967849945	2.1114464297384017	0.9049056127450293	0.9049058557649978
0.7	1.9606293541574946	1.9606288276142300	1.0557232148692008	1.0557234983924975
0.8	1.8098117115299952	1.8098112254900591	1.2065408169933725	1.2065411410199970
0.9	1.6589940689024960	1.6589936233658875	1.3573584191175440	1.3573587836474965
1	1.5081764262749962	1.5081760212417157	1.5081760212417155	1.5081764262749962

Table 8: Sixth-order HAM solution of Eq. (36) at $t = \frac{\pi}{8}$ and $h = \tilde{h}_2$ for $r \in [0, 1]$

r	$\overline{XX}(t; r)$	$\overline{X}(t; r; \tilde{h}_2)$	$\underline{X}(t; r; \underline{h}_2)$	$\underline{XX}(t; r)$
0	3.0163528525499923	3.016352845484400	0.	0.
0.1	2.8655352099224927	2.8655352032101797	0.15081764227422060	0.15081764262749964
0.2	2.7147175672949930	2.7147175609359597	0.30163528454844120	0.3016352852549993
0.34	2.5638999246674934	2.5638999186617393	0.45245292682266164	0.4524529278824989
0.4	2.4130822820399940	2.4130822763875200	0.60327056909688240	0.6032705705099985
0.5	2.2622646394124940	2.2622646341132997	0.75408821137110300	0.7540882131374981
0.6	2.1114469967849945	2.1114469918390797	0.90490585364532330	0.9049058557649978
0.7	1.9606293541574946	1.9606293495648600	1.05572349591954400	1.0557234983924975
0.8	1.8098117115299952	1.8098117072906392	1.20654113819376470	1.2065411410199970
0.9	1.6589940689024960	1.6589940650164203	1.35735878046798500	1.3573587836474965
1	1.5081764262749962	1.5081764227422000	1.50817642274220600	1.5081764262749962

In Tab. 9 there is a comparison of the mean errors by HAM, VIM and Taylor expansion method [16] (all of sixth-order) at $t = \frac{\pi}{8}$ for $r \in [0, 1]$.

Table 9: Absolute mean error for the solution of Eq. (36) at $t = \frac{\pi}{8}$, $r \in [0, 1]$, by the sixth-order HAM approximate, Taylor expansion method and VIM [16]

r	$MEr(t, r; -1)$	$MEr(t, r; \tilde{h}_2)$	Taylor method [16]	VIM [16]
0	$4.050332804705903 \times 10^{-7}$	$3.5327960556941200 \times 10^{-9}$	3.4210×10^{-6}	8.4600×10^{-7}
0.1	$4.050332806093681 \times 10^{-7}$	$3.5327959863051810 \times 10^{-9}$	3.2500×10^{-6}	8.0400×10^{-7}
0.2	$4.050332803040568 \times 10^{-7}$	$3.532795694871637 \times 10^{-9}$	3.0790×10^{-6}	7.6100×10^{-7}
0.3	$4.050332806648793 \times 10^{-7}$	$3.532795694871637 \times 10^{-9}$	2.9080×10^{-6}	7.1900×10^{-7}
0.4	$4.050332803595680 \times 10^{-7}$	$3.532795112004550 \times 10^{-9}$	2.7360×10^{-6}	6.7700×10^{-7}
0.5	$4.050332806926349 \times 10^{-7}$	$3.532794723426491 \times 10^{-9}$	2.5660×10^{-6}	6.3600×10^{-7}
0.6	$4.050332806371237 \times 10^{-7}$	$3.532794667915340 \times 10^{-9}$	2.3950×10^{-6}	5.9300×10^{-7}
0.7	$4.050332805816126 \times 10^{-7}$	$3.532794057292676 \times 10^{-9}$	2.2230×10^{-6}	5.5000×10^{-7}
0.8	$4.050332803595680 \times 10^{-7}$	$3.532794168314979 \times 10^{-9}$	2.0520×10^{-6}	5.0700×10^{-7}
0.9	$4.050332804705903 \times 10^{-7}$	$3.532793613203466 \times 10^{-9}$	1.8806×10^{-6}	4.6500×10^{-7}
1	$4.050332805816126 \times 10^{-7}$	$3.532793058091954 \times 10^{-9}$	1.7104×10^{-6}	4.2400×10^{-7}

Clearly from [Tab. 9](#) one can see that sixth-order HAM solution at the optimal value of the convergence control parameter \tilde{h}_2 is more accurate than the one by VIM and Taylor expansion method for $r \in [0, 1]$. The results in [Tabs. 7–8](#) can be summarized in [Figs. 8–9](#) as below:

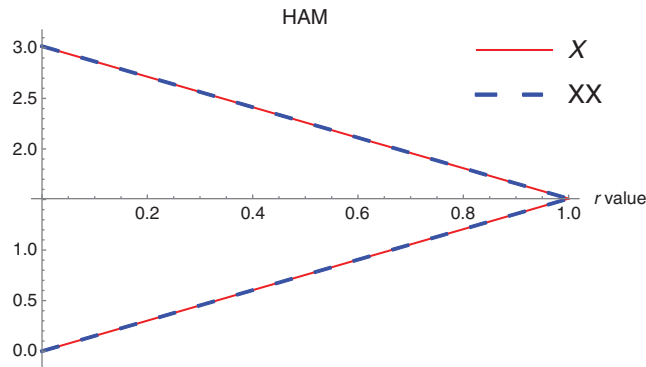


Figure 8: Sixth-order HAM for value $h = \tilde{h}_2$ and the exact solution of [Eq. \(36\)](#) at $t = \frac{\pi}{8}$ for $r \in [0, 1]$

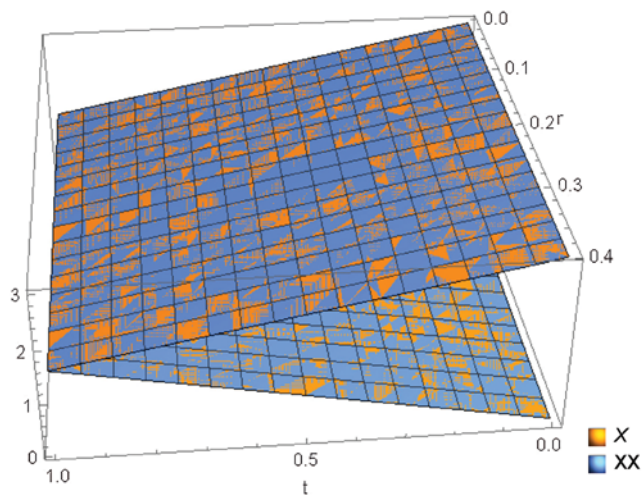


Figure 9: Sixth-order HAM solution for $h = \tilde{h}_2$ and the exact solution of [Eq. \(36\)](#) for $t \in [0, \frac{\pi}{8}]$ and $r \in [0, 1]$

Example 6.3: Find the solution of the following nonlinear fuzzy Volterra integral equation:

$$\tilde{x}(t) = \tilde{f}(t) + \int_0^t t^2(t-2s)(\tilde{x}(s))^2 ds, \tag{39}$$

where

$$\underline{f}(t; r) = (2-r)^2 \left(\frac{t^6}{6} + t^5 - t^3 + \frac{t^2}{2} \right) - \frac{t^2}{2} + rt + r,$$

$$\bar{f}(t; r) = r^2 \left(\frac{t^6}{6} + t^5 - t^3 + \frac{11t^2}{32} \right) + (2-r) \left(-(2-r) \frac{11t^2}{32} + t + 1 \right).$$

The HAM formulation of Eq. (39) is:

$$\begin{aligned} \tilde{x}_m(t; r) = \chi_{m-1} \tilde{x}_{m-1}(t; r) + \tilde{h}(r) \left[\tilde{x}_{m-1}(t; r) - \int_0^t \left(t^2(t-2s) \sum_{j=0}^{m-1} \tilde{x}_j(s; r) \tilde{x}_{m-1-j}(s; r) \right) ds \right. \\ \left. - (1 - \chi_{m-1}) \right], \end{aligned} \tag{40}$$

where the initial guess $\tilde{x}_0(t; r) = [r, 2-r]$. In this example, we introduce the residual error to show one of the HAM advantages to check the accuracy of Eq. (39):

$$\tilde{R}(t; r; \tilde{h}(r)) = \tilde{X}(t; r; \tilde{h}(r)) - \left[\underline{f}(t; r), \bar{f}(t; r) \right] - \int_a^t t^2(t-2s) \left(\tilde{X}(s; r; \tilde{h}(r)) \right)^2 ds. \tag{41}$$

The $\tilde{h}(r)$ -curves of the fifth-order fuzzy HAM upper and lower bound solutions at $r = 1$ of Eq. (39) are shown in Fig. 10.

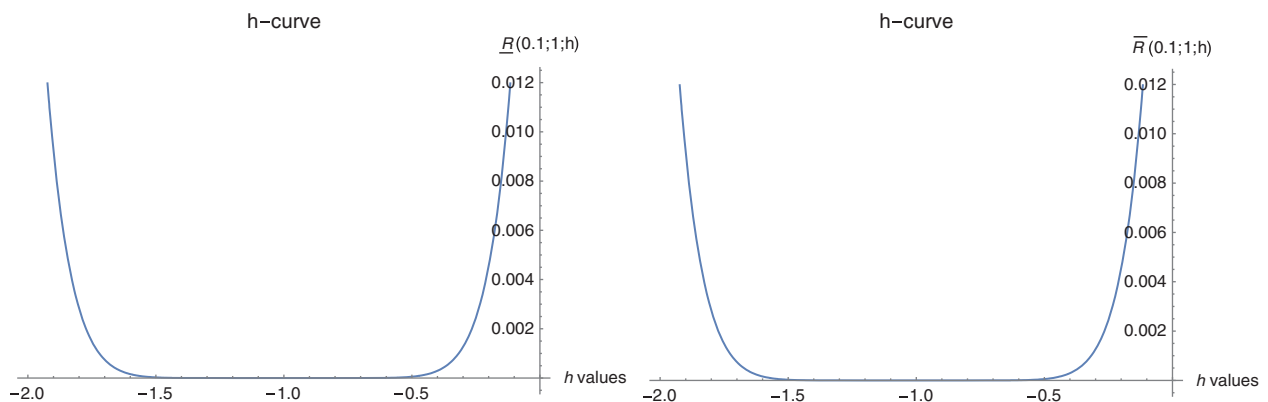


Figure 10: $\tilde{h}(r)$ -curves of fifth-order fuzzy HAM solution of Eq. (39) at $r = 1$

From Fig. 10 the valid values of \tilde{h} are in the range $-1.5 \leq \tilde{h}(1) \leq -0.6$. The only value of \tilde{h} obtained from Eq. (39) is $\tilde{h}_1 = -1.0127292274597477$ for the lower and the upper bound solutions. Therefore, Fig. 11 display the accuracy of Eq. (39) via fifth-order HAM as below:

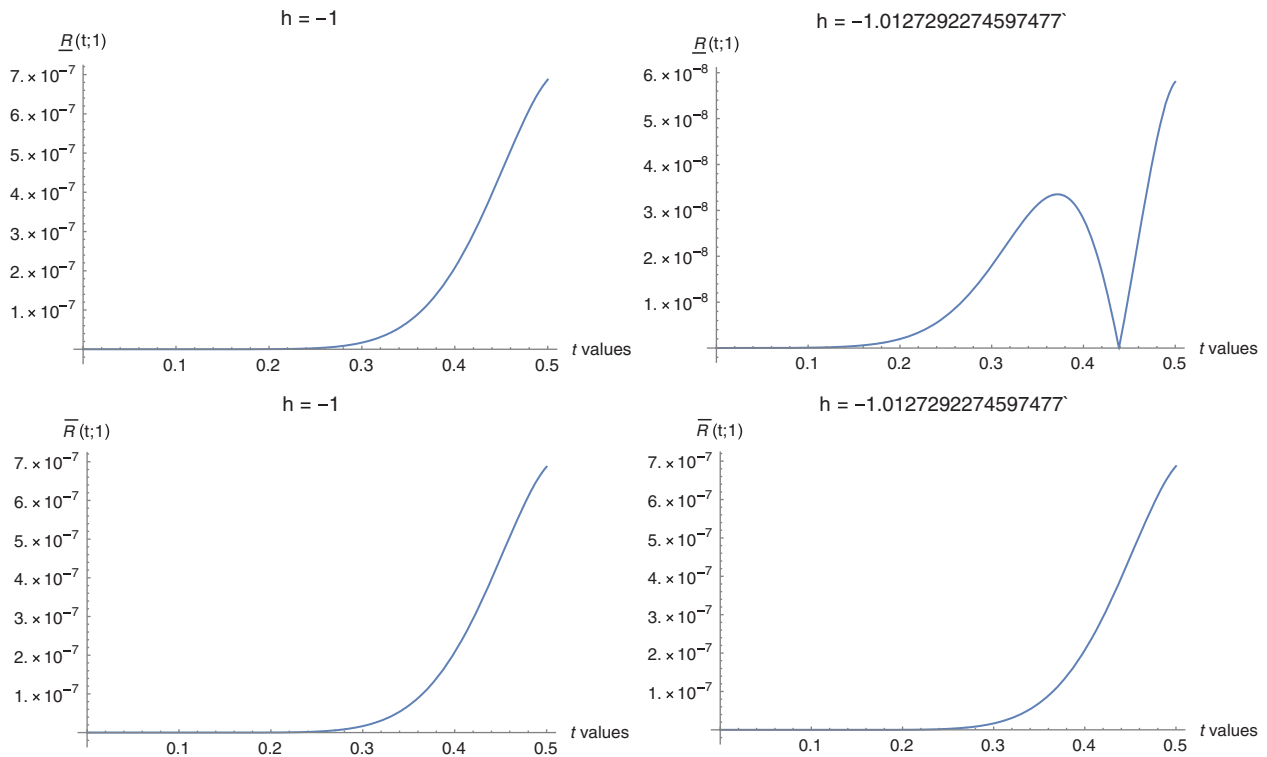


Figure 11: Fifth-order fuzzy HAM accuracy for some values of $\tilde{h}(1)$, $t \in [0, 0.5]$

Tabs. 10–13 shows the fifth-order HAM approximate solution of Eq. (39) and accuracy for different values of $r \in [0, 1]$ at $t = 0.5$ and can be summarized in Figs. 12–13 as below.

Table 10: Fifth-order HAM lower solution and accuracy for Eq. (39) at $t = 0.5$ and $h = -1$ for $r \in [0, 1]$

r	$\underline{X}(t; r; -1)$	$\underline{R}(t; r; -1)$
0	0.03128583443429885	$6.870775863809797 \times 10^{-7}$
0.2	0.30539350597446363	$6.870775863809797 \times 10^{-7}$
0.4	0.58916267633010430	$6.870775863809797 \times 10^{-7}$
0.6	0.88274732382544230	$6.870775863809797 \times 10^{-7}$
0.8	1.18630547356150950	$6.870775863809797 \times 10^{-7}$
1	1.49999930861882080	$6.870775863809797 \times 10^{-7}$

Table 11: Fifth-order HAM lower solution for Eq. (39) and accuracy at $t = 0.5$ and $h = \underline{h}_1$ for $r \in [0, 1]$

r	$\underline{X}(t; r; \tilde{h}_1)$	$\underline{R}(t; r; \tilde{h}_1)$
0	0.03128583620899258	$5.80003420846964 \times 10^{-8}$
0.2	0.30539351981441490	$5.80003420846964 \times 10^{-8}$
0.4	0.58916272787412720	$5.80003420846964 \times 10^{-8}$
0.6	0.88274746397110280	$5.80003420846964 \times 10^{-8}$
0.8	1.18630579062559000	$5.80003420846964 \times 10^{-8}$
1	1.49999994284777060	$5.80003420846964 \times 10^{-8}$

Table 12: Fifth-order HAM upper solution of Eq. (39) and accuracy at $t = 0.5$ and $h = -1$ for $r \in [0, 1]$

r	$\overline{X}(t; r; -1)$	$\overline{R}(t; r; -1)$
0	2.9954481242300500	$6.870775863809797 \times 10^{-7}$
0.2	2.6967343474932710	$6.870775863809797 \times 10^{-7}$
0.4	2.3978302489062884	$6.870775863809797 \times 10^{-7}$
0.6	2.0987381789183712	$6.870775863809797 \times 10^{-7}$
0.8	1.7994604442152753	$6.870775863809797 \times 10^{-7}$
1	1.4999993086188208	$6.870775863809797 \times 10^{-7}$

Table 13: Fifth-order HAM upper solution for Eq. (39) and accuracy at $t = 0.5$ and $h = \overline{h}_2$ for $r \in [0, 1]$

r	$\overline{X}(t; r; \tilde{h}_1)$	$\overline{R}(t; r; \tilde{h}_1)$
0	2.9954534270299886	$-5.80003420846964 \times 10^{-8}$
0.2	2.6967381357362745	$-5.80003420846964 \times 10^{-8}$
0.4	2.3978328639767135	$-5.80003420846964 \times 10^{-8}$
0.6	2.0987399093281005	$-5.80003420846964 \times 10^{-8}$
0.8	1.7994615294000882	$-5.80003420846964 \times 10^{-8}$
1	1.4999999428477704	$-5.80003420846964 \times 10^{-8}$

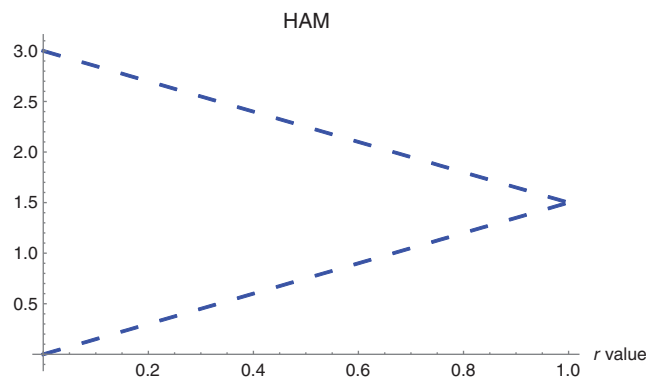


Figure 12: Fifth-order HAM solution for $h = \tilde{h}_1$ and the exact solution of Eq. (39) at $t = 0.5$, $r \in [0, 1]$

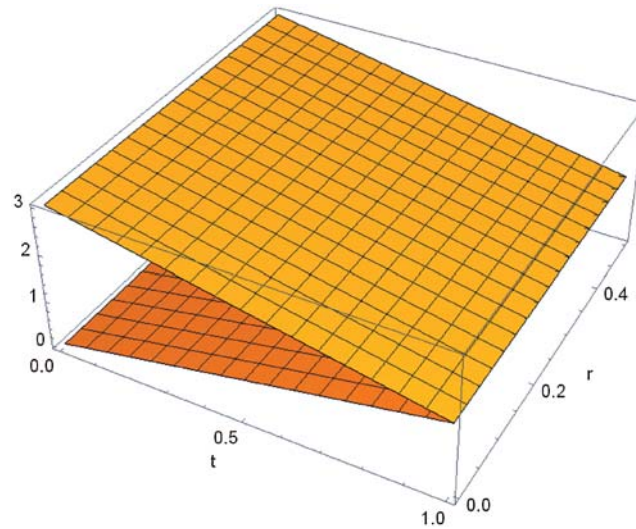


Figure 13: Fifth-order HAM solution for $h = \tilde{h}_1$ and the exact solution of Eq. (39) for $t \in [0, 0.5]$ and $r \in [0, 1]$

Example 6.4: Consider the following linear fuzzy Volterra integral equation [9]:

$$\tilde{x}(t) = [r^2 + r, 4 - r^2 - r] (\cosh(t) - \lambda \sinh^2(t)) + \lambda \int_0^x \sinh(t) \tilde{x}(s) ds, \quad (42)$$

The exact solution for Eq. (42) is given by

$$\tilde{X}\tilde{X}(t; r) = [r^2 + r, 4 - r^2 - r] \cosh(t). \quad (43)$$

The HAM formulation of Eq. (42) is:

$$\begin{aligned} \tilde{x}_m(t; r) = & \chi_{m-1} \tilde{x}_{m-1}(t; r) + \tilde{h}(r) \left[\tilde{x}_{m-1}(t; r) - \int_0^t (\sinh(t) \tilde{x}_{m-1}(s; r)) ds \right. \\ & \left. - (1 - \chi_{m-1}) \left([r^2 + r, 4 - r^2 - r] (\cosh(t) - \lambda \sinh^2(t)) \right) \right], \end{aligned} \quad (44)$$

where the initial guess is assumed to be $\tilde{x}_0(t; r) = [r^2 + r, 4 - r^2 - r]$. The $\tilde{h}(r)$ -curves of the fifth-order fuzzy HAM upper and lower bound solutions at $\lambda = 1$ and $r = 0.4$ of Eq. (42) are shown in Fig. 14.

The valid values of \tilde{h} from Fig. 14 are in the range $-1.4 \leq \tilde{h}(0.4) \leq -0.7$. From Eq. (42) the best valid values of \tilde{h} are listed in Tab. 14.

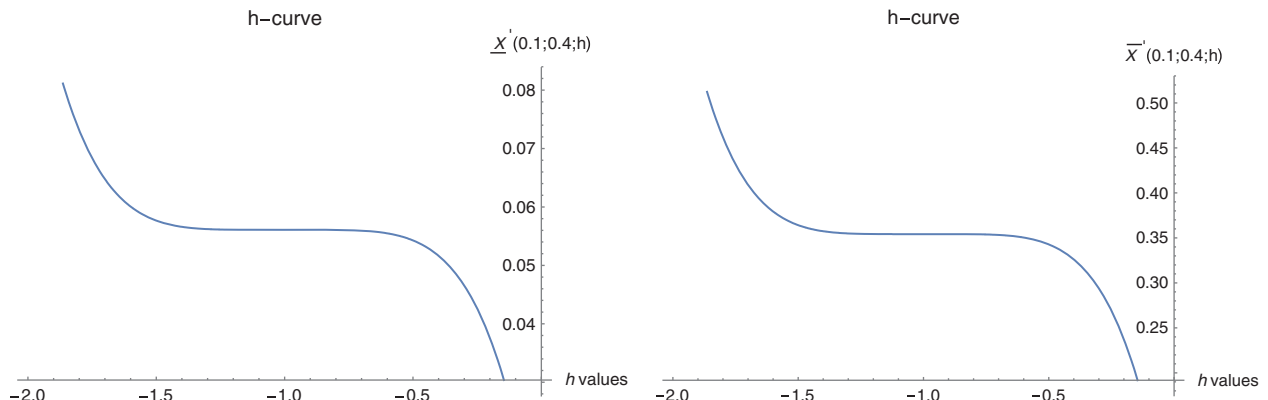


Figure 14: $\tilde{h}(r)$ -curves of the fifth-order fuzzy HAM solution accuracy of Eq. (42) at $r = 0.4$

Table 14: Best values of the convergence control parameter of the fifth-order fuzzy HAM solution of Eq. (42) at $r = 0.4$

$\underline{X}(t, \underline{h}(0.4); 0.4)$	$\underline{h}_1 \rightarrow -1.0219886874057647$	$\underline{h}_2 \rightarrow -1.0034867596086623$	$\underline{h}_3 \rightarrow -1.001243317484100$
$\overline{X}(t, \overline{h}(0.4); 0.4)$	$\overline{h}_1 \rightarrow -1.0219886871122060$	$\overline{h}_2 \rightarrow -1.0034867788302210$	$\overline{h}_3 \rightarrow -1.001243243048738$

After testing the values of \tilde{h} in Tab. 14, it turned out that the optimal value is $\tilde{h}_1 = [\underline{h}_1, \overline{h}_1]$ (see Fig. 15).

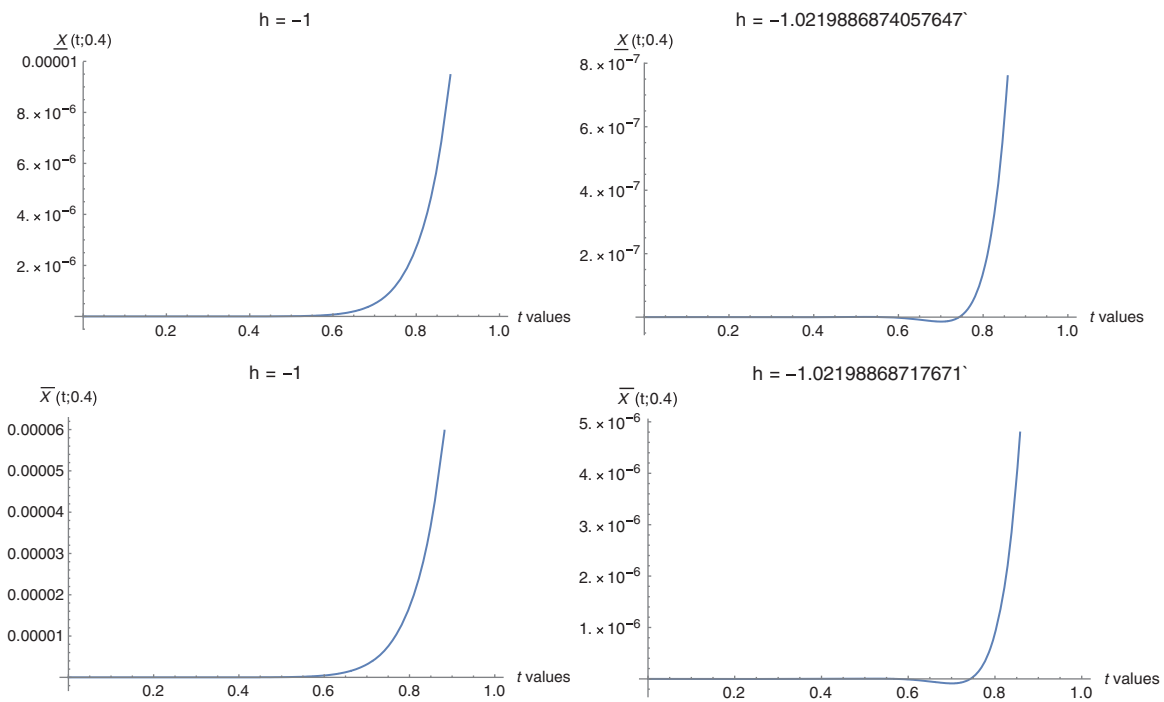


Figure 15: Fifth-order fuzzy HAM solution for some values of $\tilde{h}(0.4)$, $t \in [0, 1]$

In Tab. 15, there is a comparison of the absolute errors and the results by fifth-order HAM at \tilde{h}_1 and numerical solution via Trapezoidal quadrature formula (TQF) [9] with number of approximate iterations $N = 300$ when $\lambda = 1$ and $t = 0.5$ for different values of $r \in [0, 1]$.

Table 15: Absolute error by fifth-order HAM approximate solution of Eq. (42) for $r \in [0, 1]$ and TQF [9] at $t = 0.5$

r	$\underline{X}(0.5; r; \underline{h}_1)$	$\underline{E}(0.5; r; \underline{h}_1)$	TQF [6] lower absolute error	$X(0.5; r; \underline{h}_1)$	$E(0.5; r; \underline{h}_1)$	TQF [6] upper absolute error
0	0.	0.	0.	4.5105038560784790	4.7470×10^{-9}	9.21×10^{-8}
0.2	0.2706302313647087	2.8482×10^{-10}	6.56×10^{-8}	4.2759576555623970	4.5001×10^{-9}	1.03×10^{-8}
0.4	0.6314705398509871	6.6458×10^{-10}	1.53×10^{-7}	3.9872854087733747	4.1963×10^{-9}	9.67×10^{-7}
0.6	1.0825209254588350	1.1392×10^{-9}	2.62×10^{-7}	3.5903610694384698	3.7786×10^{-9}	8.71×10^{-7}
0.8	1.6237813881882524	1.7089×10^{-9}	3.94×10^{-7}	3.0310585912847383	3.1900×10^{-9}	7.35×10^{-7}
1	2.2552519280392396	2.3735×10^{-9}	5.47×10^{-7}	2.2552519280392396	2.3735×10^{-9}	5.47×10^{-7}

From Tab. 15 one can see that the fifth-order HAM solution at the optimal value of the convergence control parameter \tilde{h}_1 , for $r \in [0, 1]$, is more accurate than the one by TQF [9] with number of approximate iterations $N = 300$ at $t = 0.5$. The results of fifth-order HAM approximation at \tilde{h}_1 for the lower and the upper bound solutions when $\lambda = 1$ for all $r \in [0, 1]$ and $0 \leq t \leq 1$ are depicted in Figs. 16 and 17.

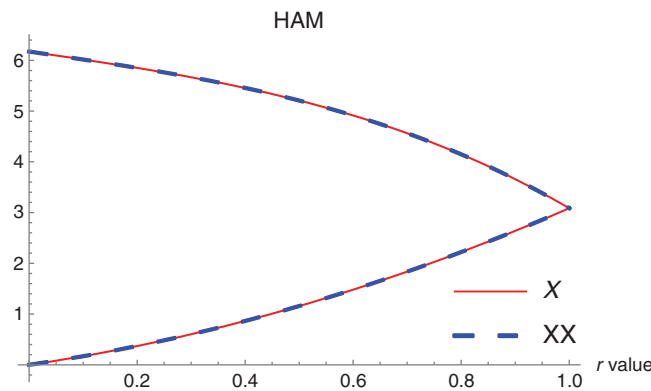


Figure 16: Fifth-order HAM solution for $h = \tilde{h}_1$, $r \in [0, 1]$, and exact solution of Eq. (42) at $t = 1$

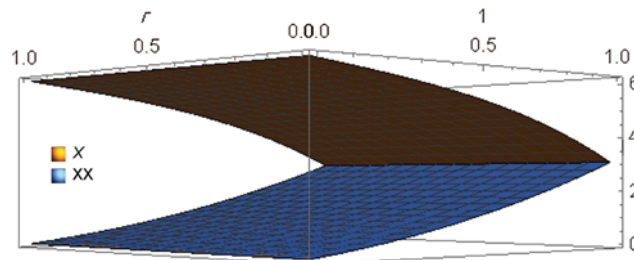


Figure 17: Fifth-order HAM solution for $h = \tilde{h}_1$, $r \in [0, 1]$, and the exact solution of Eq. (42) for $t \in [0, 1]$

7 Conclusions

This paper proposes HAM for solving fuzzy Volterra integral equation of the second kind with separable kernels. The fuzzy set theory was used to present a new formulation of HAM with application to the fuzzy Volterra integral equation of the second kind. The convergence of this approach was qualitatively discussed to find the optimal value of the convergence-control parameter. The examples presented show the potential of the method. Numerical results and graphs show that both linear and nonlinear fuzzy Volterra integral equations of the second type are well approximated by the method. Being a semi-analytical method, this approach has the advantage of lead to solutions in explicit form. The numerical experiments showed better performance of the method when compared against other approximation or numerical approaches such as VIM, the Taylor method and the Trapezoidal Quadrature Formula. Due to its accurate results, which do not violate the fuzzy sets theory solution, and a relatively low computational cost, HAM seems to be a reliable tool for solving fuzzy Volterra integral equation of the second kind. In future work, we will apply the approach to some problems in Biomathematics, such as cancer growth and epidemics.

Funding Statement: Dr. Ali Jameel and Noraziah Man are very grateful to the Ministry of Higher Education of Malaysia for providing them with the Fundamental Research Grant Scheme (FRGS) S/O No. 14188 that supported this research.

Conflicts of Interest: The authors declare that they have no conflicts of interest to report regarding the present study.

References

1. Yüzbaşı, Ş., Al-Khaled, K., Savaşaneril, N. B., Kumar, D. (2020). Introduction to the special issue on numerical methods for differential and integral equations. *Computer Modeling in Engineering & Sciences*, 123(3), 913–915. DOI 10.32604/cmescs.2020.011225.
2. Panda, S. K., Karapınar, E., Atangana, A. (2020). A numerical scheme and comparisons for fixed-point results with applications to the solutions of Volterra integral equations in dislocated extended b-metric space. *Alexandria Engineering Journal*, 59(2), 815–827. DOI 10.1016/j.aej.2020.02.007.
3. Uddin, M., Ullah, N., Inayat, S. (2020). RBF based localized method for solving nonlinear partial integro-differential equations. *Computer Modeling in Engineering & Sciences*, 123(3), 957–972. DOI 10.32604/cmescs.2020.08911.
4. Jerri, A. (1999). *Introduction to integral equations with applications*. New York, NY, USA: Wiley.
5. Tomasiello, S., Khattri S. K., Awrejcewicz, J. (2017). Differential quadrature-based simulation of a class of fuzzy damped fractional dynamical systems. *International Journal of Numerical Analysis and Modeling*, 14(1), 63–75.
6. Mohamed, R., Talaat, S., Adel, R. H., Heba, S. O. (2020). An accurate and efficient technique for approximating fuzzy fredholm integral equations of the second kind using triangular functions. *New Trends in Mathematical Sciences*, 8(2), 29–43. DOI 10.20852/ntmsci.2020.403.
7. Bica, A. M., Ziari, S. (2015). Iterative numerical method for fuzzy Volterra linear integral equations in two dimensions. *Soft Computing*, 21(5), 1097–1108. DOI 10.1007/s00500-016-2085-2.
8. Ildar, M., Aleksandr, T., Denis, N. S. (2017). Numeric solution of Volterra integral equations of the first kind with discontinuous kernels. *Journal of Computational and Applied Mathematics*, 313(15), 119–128. DOI 10.1016/j.cam.2016.09.003.
9. Saberirad, F., Karbassi, S. M., Heydari, M. (2019). Numerical solution of nonlinear fuzzy Volterra integral equations of the second kind for changing sign kernels. *Soft Computing*, 23(21), 1181–1197. DOI 10.1007/s00500-018-3668-x.

10. Salehi, P., Nejadiyan, M. (2011). Numerical method for nonlinear fuzzy Volterra integral equations of the second kind. *International Journal Industrial Mathematics*, 3, 169–179.
11. Park, J. Y., Han, H. K. (1999). Existence and uniqueness theorem for a solution of fuzzy Volterra integral equations. *Fuzzy Sets System*, 105(3), 481–488. DOI 10.1016/S0165-0114(97)00238-8.
12. Allahviranloo, T., Ghanbari, M., Nuraei, R. (2014). An application of a semi-analytical method on linear fuzzy Volterra integral equations. *Journal of Fuzzy Set Valued Analysis*, 2014, 1–15. DOI 10.5899/2014/jfsva-00161.
13. Salahshour, S., Allahviranloo, T. (2013). Application of fuzzy differential transform method for solving fuzzy Volterra integral equations. *Applied Mathematical Modelling*, 37(3), 1016–1027. DOI 10.1016/j.apm.2012.03.031.
14. Narayanamoorthy, S., Sathiyapriya, S. P. (2016). Homotopy perturbation method: A versatile tool to evaluate linear and nonlinear fuzzy Volterra integral equations of the second kind. *SpringerPlus*, 5(378), 1–16. DOI 10.1186/s40064-015-1659-2.
15. Allahviranloo, T., Khezerloo, M., Ghanbari, M., Khezerloo, S. (2010). The homotopy perturbation method for fuzzy volterra integral equations. *International Journal of Computational Cognition*, 8(2), 32–37.
16. Biswas, S., Roy, T. K. (2017). Fuzzy linear integral equation and its application in biomathematical model. *Advances in Fuzzy Mathematics*, 12(5), 1137–1157.
17. Liao, S. J. (1992). *The proposed homotopy analysis technique for the solution of nonlinear problems (Ph.D. Thesis)*. Shanghai Jiao Tong University.
18. Liao, S. J., Campo, A. (2002). Analytic solutions of the temperature distribution in Blasius viscous flow problems. *Journal of Fluid Mechanics*, 453, 411–425. DOI 10.1017/S0022112001007169.
19. Liao, S. J. (2003). An explicit analytic solution to the Thomas–Fermi equation. *Applied Mathematics and Computation*, 144(2–3), 495–506. DOI 10.1016/S0096-3003(02)00423-X.
20. Abbasbandy, S., Shivaniana, E., Vajravelu, K. (2011). Mathematical properties of h-curve in the framework of the homotopy analysis method. *Communications in Nonlinear Science and Numerical Simulation*, 16(11), 4268–4275. DOI 10.1016/j.cnsns.2011.03.031.
21. Ahmad Soltania, L., Shivaniana, E., Ezzatia, R. (2016). Convection-radiation heat transfer in solar heat exchangers filled with a porous medium: Exact and shooting homotopy analysis solution. *Applied Thermal Engineering*, 103(13–14), 537–542. DOI 10.1016/j.applthermaleng.2016.04.107.
22. Shaban, M., Shivanian, E., Abbasbandy, S. (2013). Analyzing magneto-hydrodynamic squeezing flow between two parallel disks with suction or injection by a new hybrid method based on the Tau method and the homotopy analysis method. *European Physical Journal Plus*, 128(11), 1–10. DOI 10.1140/epjp/i2013-13133-x.
23. Liao, S. J. (2009). Series solution of nonlinear eigenvalue problems by means of the homotopy analysis method. *Nonlinear Analysis: Real World Applications*, 10(4), 2455–2470. DOI 10.1016/j.nonrwa.2008.05.003.
24. Liao, S. J. (1997). A kind of approximate solution technique which does not depend upon small parameters. II. An application in fluid mechanics. *International Journal of Non-Linear Mechanics*, 32(5), 815–822. DOI 10.1016/S0020-7462(96)00101-1.
25. Liao, S. J. (2009). Notes on the homotopy analysis method: Some definitions and theorems. *Communications in Nonlinear Science and Numerical Simulation*, 14(4), 983–997. DOI 10.1016/j.cnsns.2008.04.013.
26. Vajravelu, K., van Gorder, R. A., (2012). Application of the homotopy analysis method to fluid flow problems. *Nonlinear Flow Phenomena and Homotopy Analysis*. Berlin, Heidelberg: Springer.
27. Mallory, K., van Gorder, R. A. (2014). Optimal homotopy analysis and control of error for solutions to the non-local Whitham equation. *Numerical Algorithms*, 66, 843–863. DOI 10.1007/s11075-013-9765-0.
28. van Gorder, R. A., Vajravelu, K. (2009). On the selection of auxiliary functions, operators, and convergence control parameters in the application of the homotopy analysis method to nonlinear differential equations: A general approach. *Communications in Nonlinear Science and Numerical Simulation*, 14(12), 4078–4089. DOI 10.1016/j.cnsns.2009.03.008.
29. van Gorder, R. A. (2012). Control of error in the homotopy analysis of semi-linear elliptic boundary value problems. *Numerical Algorithms*, 61(4), 613–629. DOI 10.1007/s11075-012-9554-1.

30. Samad, N., Fariborzi Araghi, M. A., Adbbasbandy, S. (2019). Finding optimal convergence control parameter in the homotopy analysis method to solve integral equations based on the stochastic arithmetic. *Numerical Algorithms*, 81(1), 237–267. DOI 10.1007/s11075-018-0546-7.
31. Khademejad, T., Khanarmuei, M. R., Talebizadeh, P., Hamidi, A. (2015). On the use of the homotopy analysis method for solving the problem of the flow and heat transfer in a liquid film over an unsteady stretching sheet. *Journal of Applied Mechanics and Technical Physics*, 56(4), 654–666. DOI 10.1134/S0021894415040136.
32. Devendra, K., Jagdev, S., Sushila (2013). Application of homotopy analysis transform method to fractional biological population model. *Romanian Reports in Physics*, 65(1), 63–75.
33. Pratibha, R., Divya, J., Saxena, V. P. (2016). Approximate analytical solution with stability analysis of HIV/AIDS model. *Cogent Mathematics & Statistics*, 3(1), 1–14. DOI 10.1080/23311835.2016.1206692.
34. Samad, N., Eisa, Z., Hasan, B. K. (2016). Homotopy analysis transform method for solving Abel's integral equations of the first kind. *Ain Shams Engineering Journal*, 7(1), 483–495. DOI 10.1016/j.asej.2015.03.006.
35. Jameel, A. F., Anakira, N. R., Alomari, A. K., Alsharo, D. M., Saaban, A. (2019). New semi-analytical method for solving two point nth order fuzzy boundary value problem. *International Journal of Mathematical Modelling and Numerical Optimisation*, 9(1), 21–31. DOI 10.1504/IJMMNO.2019.100476.
36. Jameel, A. F., Anakira, N. R., Alomari, A. K., Mahameed, M. A., Saaban, A. (2019). A new approximate solution of the fuzzy delay differential equations. *International Journal of Mathematical Modelling and Numerical Optimisation*, 9(3), 221–240. DOI 10.1504/IJMMNO.2019.100476.
37. Bodjanova, S. (2006). Median alpha-levels of a fuzzy number. *Fuzzy Sets and Systems*, 157(7), 879–891. DOI 10.1016/j.fss.2005.10.015.
38. Dubois, D., Prade, H. (1982). Towards fuzzy differential calculus. Part 3: Differentiation. *Fuzzy Set Systems*, 8(3), 225–233. DOI 10.1016/S0165-0114(82)80001-8.
39. Xixiang, Z., Weimin, M., Liping, C. (2014). New similarity of triangular fuzzy number and its application. *Scientific World Journal*, 2014, 1–7. DOI 10.1155/2014/215047.
40. Zadeh, L. A. (2005). Toward a generalized theory of uncertainty. *Information Sciences*, 172(2), 1–40. DOI 10.1016/j.ins.2005.01.017.
41. Goetschel, R., Voxman, W. (1986). Elementary fuzzy calculus. *Fuzzy Sets and Systems*, 18(1), 31–34. DOI 10.1016/0165-0114(86)90026-6.
42. Ibrahim, I., Obeng-Denteh, W., Patrick, A. A., Effah-Poku, S. (2016). Using homotopy analysis method for solving Volterra integral equations of the second kind. *Theoretical Mathematics & Applications*, 6(3), 85–100.
43. Turkyilmazoglu, M. (2011). Some issues on HPM and HAM methods: A convergence scheme. *Mathematical and Computer Modelling*, 53(9–10), 1929–1936. DOI 10.1016/j.mcm.2011.01.022.